

Transient response analysis of branched pipe systems towards a reliable skeletonization

Silvia Meniconi¹, Marco Cifrodelli², Caterina Capponi³, Huan-Feng Duan⁴, and Bruno Brunone⁵

¹Associate professor, PhD, Dipartimento di Ingegneria Civile ed Ambientale, The University of Perugia, Via G. Duranti 93, 06125 Perugia, Italy. Email: silvia.meniconi@unipg.it

²Research fellow, PhD, Dipartimento di Ingegneria Civile ed Ambientale, The University of Perugia, Via G. Duranti 93, 06125 Perugia, Italy

³Research fellow, PhD, Dipartimento di Ingegneria Civile ed Ambientale, The University of Perugia, Via G. Duranti 93, 06125 Perugia, Italy

⁴Associate professor, PhD, Hung Hom, Kowloon, SAR Hong Kong, Hong Kong Polytechnic University

⁵Professor, PhD, Member ASCE, Dipartimento di Ingegneria Civile ed Ambientale, The University of Perugia, Via G. Duranti 93, 06125 Perugia, Italy. Email: silvia.meniconi@unipg.it

ABSTRACT

In this paper the transient behavior of a single-branch pipe system (Y-system) is analyzed by means of numerical experiments in which a wide range of branch characteristics (i.e., size, location, and operating conditions) is investigated. In the executed systematic analysis, focused on the role of minor branches, the pressure signals of the Y-system have been compared with the ones of the single pipe, assumed as a reference, by means of the values of the determination coefficient, R^2 . The provided explicit relationships between R^2 and the characteristics of the branch clearly show that the actual role of the branch is determined by the combination of the characteristics more than by any single one. Such relationships are a reliable tool for the system skeletonization, i.e. they allow evaluating in which conditions a given branch can be neglected since it does not affect

significantly the transient behavior of the system. The reliability and practical implications of the proposed methodology are discussed by considering a large supply system with ten minor branches, as a case study.

INTRODUCTION

For economic reasons, transmission and irrigation pipe systems are usually branched with flow discharges at the junctions in the main pipe being equal to the users' demands. The smaller resilience with respect to looped systems, as those used for distribution networks, is balanced by an extremely large saving of money.

In branched pipe systems, the geometrical characteristics of the main pipe – i.e., material, diameter, D , and wall thickness – are often constant for the ease of management (in Fig. 1, a single-branch pipe system, often referred simply to as Y-system, is reported as a reference). On the contrary, the characteristics of the branches may vary significantly from each other according to the requested **operating conditions**. ~~As an example, the diameter of a branch, D_b , may range from quite small values up to D , according to the importance of the supplied user (hereafter, the subscript b refers quantities to the branch). Branch location along the main pipe, s_b (= distance between the branch junction and the downstream end section of the main pipe), and the length of the branch, L_b , are defined by the users' location with respect to the route of the main pipe.~~ In literature, several aspects have been examined with particular regard to Y-systems, both in steady- and unsteady-state conditions. In this paper, attention is focused on the transient behavior and the related main contributions are recalled below.

The transient response in terms of reflection and transmission coefficients of the junction between the main pipe and the branch is discussed in **Wood and Chao (1971)** for a metallic system, and in **Evangelista et al. (2015)**, **Evangelista et al. (2016)**, and **Brunone (2016)**, for a polymeric system, on the basis of accurate laboratory tests. In **Ferrante et al. (2009)**, the modalities with which pressure waves travel through a Y-system – for both a laboratory and a real case – are examined by coupling wavelet analysis with a Lagrangian model. The validity of the Network Admittance Matrix Method, as well as the relevance of the number of the measurement sections and arrangements of

the Kelvin-Voigt elements, are checked in Capponi et al. (2018), and Ferrante and Capponi (2018). The transient frequency response method for leak detection has been extended to Y-systems in Duan (2017), whereas its accuracy and sensitivity are evaluated in Duan (2018). Performance of the Inverse Transient Analysis for fault detection in Y-systems is evaluated in Kim (2016), and Capponi and Ferrante (2018) by means of numerical tests, with regard to elastic and polymeric pipes, respectively. The relevance of the branches to the transient response of the system in the time domain is shown in Meniconi et al. (2011b), and Meniconi et al. (2015), whereas in Duan and Lee (2016) the analytical expression of the frequency response function is derived within the frequency-domain approach. The effect of minor branches with a dead end on the transient behavior of a single pipe is discussed in Wang et al. (2005), and Meniconi et al. (2018).

It is worth of noting that other important aspects of transient conditions in pipe systems have been explored recently: the role of the nodal demand effect (Huang et al. 2017), the importance of field tests (Ebacher et al. 2011), and the uncertainties in parameter knowledge (Duan et al. 2010).

The mentioned contributions to literature about the transient behavior of Y-systems do not allow stating in which conditions (i.e., for a given main pipe, pressure and flow regime, and boundary conditions), a given branch significantly affects the transient behavior of the system or, in other words, when, in the skeletonized system, a given branch can be ignored without losing important features. This is due to the fact that the explored range of the branch characteristics (~~i.e., the values of D_b , s_b , and L_b~~) and operating conditions seem to be not extensive enough. In such a context, according to Jung et al. (2007), it is worth of noting that the rules used for analyzing the steady-state behavior (USEPA 2006) cannot be straightforwardly extended to transient conditions. The case of the branch with a dead end is emblematic indeed: in steady-state it is absolutely irrelevant (and then in the skeletonized system it can be ignored), whereas during transients it ~~exists~~ affects significantly the pressure waves since they double at the dead end.

According to what is discussed above, this paper focuses on the systematic analysis of the role of the characteristics and operating conditions of a branch with respect to the transient response of the system. Specifically, attention is focused on minor branches. These pipes are characterized by

a discharge smaller than the one in the main pipe, and a diameter, D_b , ranging from quite small values up to the one of the main pipe, D (hereafter, the subscript b refers quantities to the branch). The maximum value of the length of the branch, L_b , is assumed to be $0.1L$ (L = main pipe length), since usually users are located not too far from the branch junction to the main pipe. Finally, any minor branch location along the main pipe, s_b (= distance between the branch junction and the downstream end section of the main pipe) is feasible (but with, of course, $s_b < L$), since it is defined by the users' location with respect to the route of the main pipe.

The aim of this paper is to provide a reliable tool for defining a priori when the transient response of a Y-system can be assimilated to the one of the main pipe without the branch and then the branch can be ignored in the skeletonized system. Even if, as mentioned above, the below analysis is focused on transmission pipe systems, such a result could be of interest also for distribution networks. In fact, in these systems the number of the branches is so large that a reliable skeletonization procedure is attractive from the computational point of view. ~~Such a result is of valuable importance for distribution networks, where the number of branches is so large that the skeletonized system can be attractive from the computational point of view.~~ Moreover, from the practical point of view, the relevance of such an analysis is twofold. On one side, more conventional, it explores the effect of the branch in terms of the achieved extreme values. On the other side, it allows pointing out in which cases the pressure waves reflected by the branch significantly influence the pressure signal at the chosen measurement section and then they make more difficult the detection of possible faults within the transient test-based techniques for the diagnosis of pipe systems (e.g., Brunone 1999; Vitkovsky et al. 2007; Covas and Ramos 2010; Meniconi et al. 2011a; Keramat et al. 2019).

The organization of this paper is as follows. The second section introduces the numerical setup and model for simulating transients in a Y-system. The strategy for identifying which parameters affect the transient behavior of the system is illustrated in the third section. Then, the role of the branch characteristics (i.e., geometry, topology, energy dissipation mechanisms and operating conditions) is extensively described in the fourth section. In the fifth section, an efficient computational shortcut for evaluating the role of a branch is obtained on the basis of the results of the executed numerical

tests. Finally, after having discussed a practical application of the proposed procedure, conclusions are drawn in the last section.

THE INVESTIGATED SYSTEM AND GOVERNING EQUATIONS

As mentioned above, attention is focused on a Y-system (Fig. 1), with an upstream supply reservoir, SR, and a maneuver valve, EV, discharging in the air, installed at the downstream end of the main pipe. At a distance s_b from EV, a minor branch of length L_b and diameter D_b connects to the main pipe. During the steady-state conditions, the valve EV is open and the initial mean flow velocity in the main pipe downstream of the branch, d , and in the branch are $V_{0,d}$ and $V_{0,b}$, respectively, with the subscripts 0 and d referring quantities to the initial conditions and main pipe downstream of the junction, respectively. Transients are generated by the complete and instantaneous closure of EV. In the below analysis, the pressure signal at section M, immediately upstream of EV, is assumed as representative of the transient response of the system.

In the executed numerical experiments, the classical water hammer equations in elastic pipes, integrated within the method of the characteristics, are considered (Ghidaoui et al. 2005):

$$\frac{\partial H}{\partial s} + \frac{V}{g} \frac{\partial V}{\partial s} + \frac{1}{g} \frac{\partial V}{\partial t} + J = 0 \quad (1)$$

being the momentum equation, with H = piezometric head, V = mean flow velocity, s = spatial co-ordinate, t = time, g = acceleration due to gravity, J = total friction term ($= 4\tau_w/\rho g D$, with τ_w = wall shear stress, and ρ = fluid density), and

$$\frac{\partial H}{\partial t} + \frac{a^2}{g} \frac{\partial V}{\partial s} = 0 \quad (2)$$

being the continuity equation, with a = pressure wave speed. In Eq. (1), τ_w is regarded as the sum of two components:

$$\tau_w = \tau_{w,s} + \tau_{w,u} \quad (3)$$

where $\tau_{w,s} = f\rho V^2/8$, with f = friction factor, is the steady-state component, and $\tau_{w,u}$, the unsteady-

state component, is evaluated by means of an Instantaneous Acceleration-Based model (Brunone and Morelli 1999; Vardy and Brown 1996):

$$\tau_{w,u} = \frac{\rho k_u D}{4} \left(\frac{\partial V}{\partial t} + \text{sign}(V) \frac{\partial V}{\partial s} \right) a \frac{\partial V}{\partial s} \quad (4)$$

with k_u = unsteady friction coefficient. The user demand at the branch is simulated by means of the fixed orifice equation within a pressure driven approach (Jung et al. 2009).

SIMULATION PROCEDURE

MATERIALS AND METHODS

To identify the quantities affecting the pressure signal at section M during the transients, the following functional dimensional relationship has been considered:

$$H(t) = f \left(\underbrace{(k, \rho, \Theta)}_{\text{fluid}}; \underbrace{(A, L, a, f, k_u)}_{\text{main pipe characteristics}}; \underbrace{(V_{0,d}, H_{SR})}_{\text{main pipe initial condition}}; \underbrace{(A_b, L_b, s_b, a_b, f_b, k_{u,b}, V_{0,b})}_{\text{branch}}; \underbrace{(T, \delta)}_{\text{maneuver}}; \underbrace{(t_{stop})}_{\text{observation}} \right) \quad (5)$$

where quantities are logically grouped by means of brackets. In Eq. (5), k (= bulk modulus of elasticity), ρ , and Θ (= temperature) take into account the characteristics of the fluid; A (= main pipe cross-sectional area), L , a , f , and k_u allow pointing out the effect of the main pipe characteristics and material, with the related steady- and unsteady-state friction losses; $V_{0,d}$ and the piezometric head at the supply reservoir, H_{SR} , take into account the main pipe initial and boundary conditions; the geometrical characteristics and topology (i.e., A_b , L_b , and s_b), material and friction losses (i.e., a_b , f_b , and $k_{u,b}$), as well as initial conditions ($V_{0,b}$) define the branch completely. The characteristics of the maneuver which causes the transient are the maneuver duration, T , and the dimensionless valve opening, δ ($\delta = 0$ and $\delta = 1$ indicating the valve fully closed and open, respectively); moreover, the time of observation, t_{stop} , is included as a crucial feature of the simulated transients. As mentioned, in order to minimize the effect of the maneuver, an instantaneous one is considered ($T = 0$), as well

as to maximize the effect of the branch only the first fifteen characteristics times are analyzed ($t_{stop} = 15 \theta$, with $\theta = 2L/a$ being the main pipe characteristic time).

In the numerical experiments below, according to real system characteristics, a metallic main pipe with DN500, $A = 0.193 \text{ m}^2$, $L = 1000 \text{ m}$, $f = 0.0137$, $a = 1000 \text{ m/s}$, $V_{0,d} = 1 \text{ m/s}$ and H_{SR} as a constant ($= 100 \text{ m}$) is considered. To explore the role played by real minor branches, the branch nominal diameter ranges between DN50 and DN500, L_b and s_b range between 1.5 m to 100 m, and between 100 m and 900 m, respectively. Moreover, both inactive and active branches are considered with $V_{0,b}$ ranging between 0 and 2 m/s. Finally, without loss of generality, the steady- and unsteady-state friction coefficients, and pressure wave speed of the branch are assumed equal to the ones of the main pipe.

To evaluate the relevance of the energy dissipation mechanisms during transients, two different model assumptions are made: i) the simplest model (FL) with the classical frictionless water hammer equations ($\tau_w = 0$), and ii) the complete model (UF), with both the steady and unsteady-state friction terms.

The obtained numerical results have been synthesized by means of the following dimensionless quantities:

$$h = \frac{(H - H_0)}{\Delta H_{AJ}} \quad (6)$$

$$\tau = t/\theta \quad (7)$$

$$\alpha = A_b/A \quad (8)$$

$$\lambda = L_b/L \quad (9)$$

$$\sigma = s_b/L \quad (10)$$

$$v = V_{0,b}/V_{0,d} \quad (11)$$

where $\Delta H_{AJ}(= aV_{0,d}/g)$ is the Allievi-Joukowski overpressure, and the dimensionless area, α , length, λ , location, σ , and steady-state velocity, v , characterize the branch with respect to the main

pipe. Consequently, Eq. (5) can be rewritten in dimensionless terms as:

$$h(\tau) = f'(\alpha, \lambda, \sigma, \nu) \quad (12)$$

As mentioned above, attention is focused on minor branches. Accordingly, α will range from 0.01 to 1, λ from 0.001 to 0.1, σ from 0.1 to 0.9, and ν from 1 to 2.

The relevance of the characteristics and **operating conditions** of the branch during transients with respect to the case of a single pipe, assumed as a reference, has been quantified by means of the coefficient of determination:

$$R^2 = 1 - \frac{\sum_i \left(h_{b,m,i} - h_{SP,m,i} \right)^2}{\sum_i \left(h_{b,m,i} - \overline{h_{b,m}} \right)^2} \quad (13)$$

where the subscripts SP and m indicate the single pipe, and the used model (with $m = FL$, for the frictionless model, and $m = UF$, for the complete model), respectively, whereas $\overline{h_b}$ is the mean value over t_{stop} . According to Eq. (13), the larger R^2 , the smaller the difference between the single pipe and the Y-system, and then, the influence of the branch on the pressure signal.

THE ROLE OF THE GEOMETRY AND TOPOLOGY CHARACTERISTICS OF THE BRANCH

The role of the geometry and topology

To capture and emphasize the role of the branch location and size, the classical frictionless water hammer equations (FL model) have been used, as well as an inactive branch with the downstream end section behaving as a dead end (i.e., $\nu = 0$) has been assumed (hereafter such a system is referred to as IB): first the effect of the single characteristics and then the one of their combination is examined. Successively, the role of the energy dissipation mechanisms and **operating conditions of the branch** is discussed.

For given dimensionless branch area, α , and location, σ , the influence of the branch dimensionless length, λ , is clearly evidenced in Figs. 2a and 2b. In these figures, the pressure signals for $\alpha = 0.282$ and $\sigma = 0.5$ but for two different values of λ ($= 0.02, 0.08$) are reported and compared to

the single pipe (SP) case. Such pressure signals indicate that the larger λ , the larger the shift and amplitude of the pressure peaks, with respect to the SP case, i.e., the smaller R_{IB}^2 .

The role played by the branch dimensionless area, α , for given length λ (e.g., $\lambda = 0.07$), and location, σ (e.g., $\sigma = 0.5$) is clearly pointed out in Figs. 2c and 2d, where the IB pressure signals differ progressively from the SP ones with α rising from 0.012 to 1. In other words, the larger the branch dimensionless area, α , the smaller R_{IB}^2 , i.e., the larger the impact of the branch.

Figs. 2e and 2f clearly highlight that the IB pressure signals referring to the same value of α ($= 0.282$) and λ ($= 0.07$) show the larger peaks and shift for the smaller σ with respect to the SP ones. This means that the smaller the distance between the branch and the maneuver valve, the larger the effect of the branch.

~~The role of the combination of the branch characteristics~~

The role of the combination of the branch dimensionless area, α , and length, λ , in terms of R_{IB}^2 values, can be deduced from Fig. 3 curves obtained for a given value of the dimensionless location, σ ($= 0.5$). Precisely, such curves indicate that the smaller α , the smaller the influence of λ . **This means that if the branch area is significantly smaller than the one of the main pipe, then the influence of the branch length reduces.**

From the practical point of view, to decide if a branch can be neglected, a threshold value, R^* , must be chosen. Such a value depends mainly on the required level of accuracy of the simulation and the importance of the system. If, as an example, it is assumed $R^* = 0.90$, the branch can be neglected, for any values of λ , when $\alpha \leq 0.047$. Vice versa, for $\alpha \geq 0.1047$, the influence of λ increases: the larger the branch length, the smaller R_{IB}^2 , i.e., the larger the role played by the branch in the transient response of the system.

The combined role of the dimensionless length, λ , and location of the branch, σ , is highlighted in Fig. 4. This plot confirms that, for a given σ , the larger the branch length, the smaller R_{IB}^2 . Moreover, for the smaller values of λ (≤ 0.02), the influence of σ is negligible and in fact R_{IB}^2 is always larger than 0.91. Vice versa, for larger λ , such an influence is more important, with a smaller value of R_{IB}^2 for a smaller σ . **This means that if the branch length is larger, then the influence of its**

location increases.

Finally, Fig. 5 shows R_{IB}^2 vs. σ for a given λ ($= 0.05$) and different values of α . It can be pointed out that for the smaller values of α , the branch location is irrelevant: in fact, for $\alpha \leq 0.282$, R_{IB}^2 is almost constant. Vice versa, for the larger α , on the whole R_{IB}^2 decreases with σ , i.e., the larger the distance of the branch from the end valve EV, the less relevant its influence. However, a singularity in the behavior of R_{IB}^2 vs. σ for a given α occurs when $\sigma = 0.5$. This is due to a particular combination of the pressure waves reflected by the supply reservoir, the branch, and the already closed end valve EV which strengthens the shift in the inactive branch (IB) system with respect to the single pipe (SP).

The role of the energy dissipation mechanisms

To take into account the effect of the energy dissipation mechanisms, the friction losses have been evaluated by means of Eq. (3), with the only parameter, k_u , evaluated according to literature (Vardy and Brown 1996). As pressure signals of Fig. 6, representative of all the executed tests, clearly show, the performance of the complete model (UF model) implies a better agreement of the simulated damping of the pressure peaks between the single pipe (SP) and inactive branch pipe system (IB). In other words, the effect of the branch becomes less severe when the actual transient energy dissipation mechanisms are taken into account.

The role of the operating conditions

To highlight the role of the operating conditions of the branch, beyond the inactive pipe system (IB), three different dimensionless steady-state velocities ($v = 1, 1.5$ and 2) have been considered for the active pipe system (AB). As an example, in Fig. 7 the case of a given value of α ($= 0.398$) is reported. This plot shows that, for each σ , the role of λ is crucial for the case of the inactive branch (IB). This feature reflects in the fact that for $v = 0$ (IB case) R_{IB}^2 varies significantly with λ , for any given σ . As a consequence, a huge dispersion of empty circles can be observed in Fig. 7: as an example, in the case of $\sigma = 0.5$, $R_{IB}^2 = 0.98$ for $\lambda = 0.0015$, and $R_{IB}^2 = 0.57$ for $\lambda = 0.1$. Precisely, R_{IB}^2 varies significantly with λ (e.g., in the case of $\sigma = 0.5$, $R_{IB}^2 = 0.98$ for $\lambda = 0.0015$, and $R_{IB}^2 = 0.57$ for $\lambda = 0.1$). On the contrary, for the active branch ($v > 0$), the larger v the more negligible

the role of λ : as an example, in the case of $\nu = 2$ and $\sigma = 0.5$, $R_{AB}^2 = 0.389$ for $\lambda = 0.0015$, and $R_{AB}^2 = 0.384$ for $\lambda = 0.1$. This means that, for the active (open) branch the role of the length is not so crucial because of the smaller reflection of the pressure waves at the downstream active end section. On the contrary, for the inactive branch, the doubled reflection at the downstream dead end emphasize the role of λ .

AN EFFICIENT COMPUTATIONAL SHORTCUT FOR EVALUATING THE ROLE OF A BRANCH

In the above analysis, the effect of a branch on the transient behavior of the system has been evaluated by comparing the transient response of the single pipe to the one of the branched system both obtained by integrating numerically the water hammer equations (numerical model approach). Another way for evaluating the role of the branch is to take into account the obtained results and to use the provided curves of the determination coefficient as a function of the branch characteristics, as it will be illustrated below. To speed up the procedure, separately for the two cases of inactive (IB) and active (AB) branch, an option could be to express R^2 as a function of the branch characteristics by using a correlation function. Within an engineering approach, the choice of the proper correlation function may be guided by two main factors: i) the behavior of the obtained curves (i.e., those in the Figs. 3, 4, 5, and 7 plots), and ii) a cost-benefit analysis (i.e., the proposed relationship should be much easier and less time consuming to use with respect to the numerical model approach). In both the IB and AB cases, as a good compromise in terms of simplicity and acceptable rigor, the multiple linear regression approach – a tool available in most of engineering software – is the first option to be verified. Depending on the performance of such a working hypothesis, possible more adequate – as well as more sophisticated – models can be used.

As a first attempt, for the IB case, if no interaction terms are included in the regression, the following equation is obtained:

$$R_{IB}^2 = 1.0371 - 0.4019\alpha - 2.7765\lambda + 0.1417\sigma \quad (14)$$

Such an equation allows clearly pointing out the dependance of R_{IB}^2 on the variables of the model. Specifically, the smaller α , or λ , the larger R_{IB}^2 , with a clear predominance of λ ; moreover, on a scale of importance, the relevance of σ is the smallest one. However, since Eq. (14) implies a quite large (= 0.38) maximum absolute residual, there is the need to include also the interaction terms in the regression model. This is an obvious consequence of the well-known mechanisms of interaction between the pressure waves in a complex pipe system, clearly pointed out by curves of Figs. 3, 4, and 5. Accordingly, the following relationship has been obtained:

$$R_{IB}^2 = 0.9868 + 0.0161\alpha - 0.0501\lambda - 0.0050\sigma - 13.8191\alpha\lambda + \\ - 0.0922\alpha\sigma - 0.7203\lambda\sigma + 12.8042\alpha\lambda\sigma \quad (15)$$

Precisely, Eq. (15) shows that the larger both the length and the cross-sectional area of the branch the larger its importance; vice versa, as already highlighted in Figs. 4 and 5, the larger σ , the larger R_{IB}^2 even for the larger values of λ and α . The reliability of Eq. (15) is confirmed in Fig. 8a, where the values of R_{IB}^2 (indicated by grey circles) and the ones given by the numerical simulation within the UF model (black circles) are reported vs. α and $\lambda + \sigma$. The latter sum of parameters, representing the dimensionless travel time of the pressure waves to arrive to the branch downstream end, allows taking into account the topology of the system on the whole. The error of the fitting slightly increases with α , but it remains within acceptable limits, i.e., with a maximum of 0.15 and an average value of 0.03. Eq. (15) implies much smaller residuals (median absolute value = 0.019; maximum absolute value = 0.15), which have a random pattern, clearly highlighted in Fig. 8b, that supports the adopted linear model. Moreover, Eq. (15) confirms the fact that in R_{IB}^2 the influence of the single parameters, α , λ , and σ is quite marginal whereas there is a clear predominance of their combinations. Precisely, α and λ play the main role with the largest value of the interaction term coefficient (= -13.8191) of their product, with respect to σ . This means that the larger both the length and the cross-sectional area of the branch, the smaller R_{IB}^2 , i.e. the larger the branch importance. Such a term is partially smoothed by the $\alpha\lambda\sigma$ one (= 12.8042), in which the smaller

but not negligible effect of σ is highlighted, also for the largest values of α and λ . For the sake of completeness, it must be pointed out that only in 6 cases among the about 700 executed numerical experiments, Eq. (15) gives negative values of R_{IB}^2 ; this happens for $\alpha = 1$, when σ ($= 0.1, 0.2, 0.3$) is very small and λ ($= 0.08, 0.1$) very large.

From the practical point of view, Eq. (15) allows evaluating a priori the importance of the branch, and eventually proceed towards the skeletonization of the system.

As for the IB case, also for the active branch pipe system (AB), firstly the simplest approach, including only α , σ , and ν has been followed:

$$R_{AB}^2 = 0.8117 - 0.6529\alpha - 0.0999\nu + 0.4779\sigma \quad (16)$$

The relative branch length, λ , is not included in the Eq. (16), since, as demonstrated in Fig. 7, the importance of the branch length drastically reduces for increasing ν . Moreover, such an equation shows that the larger α or ν , with a clear predominance of α , or the smaller σ , the smaller R_{AB}^2 . Since Eq. (16) implies very large residuals (maximum absolute value = 0.43), the more refined approach, with the combination terms, has been considered:

$$R_{AB}^2 = 0.7978 + 0.2261\sigma + 0.1059\alpha + 0.0527\nu - 0.2667\alpha\sigma + \\ - 0.0628\sigma\nu - 1.112\alpha\nu + 1.0791\alpha\sigma\nu \quad (17)$$

The results given by Eq. (17), based on about 2000 executed numerical experiments, are shown in Fig. 9a, where the values of R_{AB}^2 are compared to the ones obtained by the numerical simulation within the UF model in the case, as an example, of $\nu = 1$. The goodness of the fitting (the maximum absolute value is 0.19, whereas its median absolute value is 0.04) is confirmed by the small values of the residuals, as shown in Fig. 9b., for $\nu = 1$

According to Eq. (17), in R_{AB}^2 there is a clear predominance of the combinations of α , ν , and σ , whereas the influence of the single parameters is quite marginal. Precisely, in this case, α and ν play the main role with the largest value of the interaction term coefficient ($= -1.112$) of their product,

with respect to σ . This means that the larger both the velocity and the cross-sectional area of the branch, the smaller R_{AB}^2 , i.e. the larger the branch importance. Such a term is partially smoothed by the $\alpha v \sigma$ one ($= 1.0791$), in which the smaller but not negligible effect of σ is highlighted, also for the largest values of α and v . The coefficients of Eq. (17) emphasize the larger smoothness of the phenomenon with respect to the inactive branch pipe system (IB) and highlight the importance of both the single parameter α , and the combination of α and σ on the behavior of R_{AB}^2 . As an example, a larger branch area—eventually combined with a smaller distance of the branch from EV—emphasizes the branch effect on the pressure signal with respect to the SP system. As shown in the below practical application, Eq. (17) can be a practical tool for pipe system skeletonization in the case of active branches.

A PRACTICAL APPLICATION

To check the performance of the proposed methodology for the pipe system skeletonization, a case study very close to a real tree-type pipe system operating in the Umbria region (Italy) is discussed. The considered network (Fig. 10) consists of an iron main pipe (DN500, $L = 30288$ m) supplied by a reservoir, with ten minor branches, whose characteristics are reported in Table 1. As in real cases, the downstream mean flow velocity in the main pipe, $V_{0,d}$, is quite small ($= 0.2$ m/s) to avoid dangerous water hammer phenomena; all branches are active but one (# 6). The transient is generated by the total and fast closure of the downstream end valve EV. The skeletonization of the system has been carried out by assuming that Eqs. (15) and (17) can be used notwithstanding the considered system is not a Y-system but a tree-type one. As shown in Fig. 11a, if a threshold value $R^* = 0.9$ is chosen, there are four branches (# 1, 2, 4, and 6, highlighted in bold) for which the determination coefficient is larger than R^* , and then can be eliminated. The reliability of this approach is confirmed by the pressure signals reported in Fig. 12, where the transient response of the skeletonized system is almost indistinguishable from the one of the real case: this is true both in the short and the long term. On the contrary, if $R^* = 0.8$ is assumed, a larger number of branches (six: # 1, 2, 4, 5, 6, and 10) can be neglected (Fig. 11a). For this value of R^* , larger differences can be noted in the pressure signals (Fig. 12); however, the main features of the real case are well

captured. As a result, it can be affirmed that, for the considered case, the interaction between the single branches is negligible and then Eqs. (15) and (17) can be used. On the contrary, if the real system is considered as a single pipe (SP), the numerical model results are quite poor, as shown in Fig. 12. This qualitative analysis is confirmed by the values of the determination coefficient:

$$R_{RS}^2 = 1 - \frac{\sum_i \left(h_{real,i} - h_{sk,i} \right)^2}{\sum_i \left(h_{real,i} - \overline{h_{real}} \right)^2} \quad (18)$$

where the subscripts *real* and *sk* indicate the real system and the skeletonized one, respectively. In fact, as shown in Fig. 11b, $R_{RS}^2 = 0.76$ for the SP system, 0.999, and 0.98 for the skeletonized one in the case of $R^* = 0.9$, and 0.8, respectively. Moreover, the advantage of using the system skeletonized by Eqs. (15) and (17) reflects in the large saving in terms of computational time, as shown in Fig. 11b. In this figure the relative computational time, t_{comp}^* , is considered:

$$t_{comp}^* = t_{comp} / t_{comp,SP} \quad (19)$$

with t_{comp} , and $t_{comp,SP}$ referring to the the different considered cases and the single pipe (SP), respectively. It is worth of noting that for the real system t_{comp}^* (= 1.214) is larger than the one for SP system (=1); this value strongly reduces for the skeletonized systems (= 1.089, and 1.080 for $R^* = 0.9$ and 0.8, respectively). In other words, it is assumed that the interaction between the single branches is negligible. This is a very strong assumption, but as shown below, the results are quite encouraging. As a reference, in Fig. 12 the transient response of the real system with all branches is reported, as well as the single pipe case (SP). The reduction of the computational time of the SP case with respect to the real case is equal to 21%, but this implies a quite small value of the determination coefficient (= 0.76). As a consequence, such a very rough skeletonization is not acceptable. On the contrary, if the proposed methodology is applied—with a threshold value $R^* = 0.9$ —branches # 1, 2, 4, and 6 (highlighted in bold in Table 1 can be neglected, and the

transient response of the skeletonized system captures the main features of the real case, as shown in Fig.12. The related determination coefficient is equal to 0.99, with an appreciable reduction of the computational time (= 11 %).

CONCLUSIONS

This paper focuses on the transient behavior of a single-branch pipe system (Y-system) by analyzing the effect of the characteristics of the branch (i.e., size, location, and **operating conditions**). With respect to literature, by means of numerical experiments, a wide range of cases is explored with the aim of identifying when the role of the branch can be neglected. **In the provided analysis, two successive steps have been taken concerning the inactive (IB) and the active (AB) branch, respectively. In both steps, the pressure signals of the Y-system have been compared with the ones of the single pipe assumed as a reference. As a metrics for evaluating the accuracy of the skeletonization, the determination coefficient, R^2 , has been considered: the smaller R^2 , the larger the importance of the branch.**

The results obtained for the inactive branch show that: i) for given branch cross-sectional area (α) and location (σ), the larger the length (λ), the larger the branch role (i.e., the smaller R_{IB}^2), ii) for given branch location and length, the larger the area, the larger the branch impact, and iii) for given branch area and length, the smaller the distance from the measurement section (σ), the larger the branch importance.

The numerical experiments executed for the active (AB) branch, for which the role of the operating conditions has been examined, indicate that, with respect to the IB case, the importance of the branch length reduces but not the one of its cross-sectional area and location.

With the aim of providing an efficient computational shortcut for evaluating the role of a branch, for both the inactive and active case, a multiple linear regression linking R^2 to the branch characteristics has been proposed. In both cases, the very important result is that the combination and not a single characteristic plays a very crucial role in the transient response of the system. This result is perfectly in line with the well-known mechanisms of propagation of pressure waves in pressurized pipe systems.

The provided explicit relationships between the determination coefficient and the branch characteristics allow evaluating preliminarily the effect of the branch in unsteady-state conditions. Specifically, once the branch geometry, topology and operating conditions are known, its inclusion in the simulation can be established a priori for a given accuracy (i.e., a threshold value, R^* of R^2). The proposed methodology is applied to a real system with several minor branches with encouraging results. The efficiency in terms of computational time of the numerical simulations executed for the skeletonized system instead for the real one is also shown. Based on the obtained results, the suggested relationships candidate as a reliable tool for the skeletonization of a Y-system in transient conditions. In the provided analysis, two successive steps have been executed. In the first step, for an inactive branch the effect of the size and location has been isolated by using a frictionless model; successively, both steady and unsteady friction losses have been included. In the second step, the role of the branch operating conditions has been examined. In both steps, the pressure signals of the Y-system have been compared with the ones of the single pipe assumed as a reference. As a metrics for evaluating the accuracy of the skeletonization, the determination coefficient, R^2 , has been considered.

For both the inactive and active branches, a multiple linear regression linking R^2 to the branch characteristics has been proposed. In both cases, the most important result is that not only the single characteristics but also their combination determine the actual role of the branch. Precisely, the relevance of the inactive branch depends on the combination of its length and size, but also its location with respect to the section where the transient is originated. Vice versa, for an active branch, the different boundary condition at the branch end section reduces significantly the importance of the length of the branch, but not the one of its size and location.

The provided explicit relationships between the determination coefficient and the branch characteristics allow evaluating preliminarily the effect of the branch in unsteady-state conditions. Specifically, once the branch geometry, topology and operating conditions are known, its inclusion in the simulation can be established a priori for a given accuracy (i.e., a threshold value, R^* of R^2). The proposed methodology is applied to a real system with several branches with encouraging

results. Based on the obtained results, the suggested relationships candidate as a reliable tool for the skeletonization of a single branch pipe system in transient conditions.

DATA AVAILABILITY STATEMENT

All data, models, or code generated or used during the study are available from the corresponding author by request.

ACKNOWLEDGMENTS

This research has been funded by the Hong Kong (HK) Research Grant Council Theme-Based Research Scheme and the HK University of Science and Technology (HKUST) under the project “Smart Urban Water Supply System (Smart UWSS)”. Support from Fondazione Cassa Risparmio Perugia (project #2017.0234.021), and University of Perugia is acknowledged.

REFERENCES

- Brunone, B. (1999). “A transient test-based technique for leak detection in outfall pipes.” *Journal of Water Resources Planning and Management, ASCE*, 125(5), 302–306.
- Brunone, B. (2016). “Discussion of “Hydraulic transients in viscoelastic branched pipelines” by S. Evangelista, A. Leopardi, R. Pignatelli, and G. de Marinis.” *Journal of Hydraulic Engineering*, 142(8), 07016005.
- Brunone, B. and Morelli, L. (1999). “Automatic control valve induced transients in operative pipe system.” *Journal of Hydraulic Engineering*, 125(5), 534–542.
- Capponi, C. and Ferrante, M. (2018). “Numerical investigation of pipe length determination in branched systems by transient tests.” *Water Science and Technology: Water Supply*, 18(3), 1062–1071.
- Capponi, C., Ferrante, M., Zecchin, A. C., and Gong, J. (2018). “Experimental validation of the admittance matrix method on a y-system.” *Journal of Hydraulic Research*, 56(4), 439–450.
- Covas, D. and Ramos, H. (2010). “Case studies of leak detection and location in water pipe systems by Inverse Transient Analysis.” *Journal of Water Resources Planning and Management*, 136(2), 248–257.

- Duan, H. (2017). “Transient frequency response based leak detection in water supply systems with branched and looped junctions.” *Journal of Hydroinformatics*, 19(1), 17–30.
- Duan, H. (2018). “Accuracy and sensitivity evaluation of TFR method for leak detection in multiple-pipeline water supply systems.” *Water Resources Management*, 32, 2147–2164.
- Duan, H. and Lee, P. J. (2016). “Transient-based frequency domain method for dead-end side branch detection in reservoir pipeline-valve systems.” *Journal of Hydraulic Engineering*, 142(2), 04015042.
- Duan, H.-F., Tung, Y.-K., and Ghidaoui, M. S. (2010). “Probabilistic analysis of transient design for water supply systems.” *Journal of Water Resources Planning and Management*, 136(6), 678–687.
- Ebacher, G., Besner, M.-C., Lavoie, J., Jung, B. S., Karney, B. W., and Prevost, M. (2011). “Transient modeling of a full-scale distribution system: comparison with field data.” *Journal of Water Resources Planning and Management*, 137(2), 173–182.
- Evangelista, S., Leopardi, A., Pignatelli, R., and de Marinis, G. (2015). “Hydraulic transients in viscoelastic branched pipelines.” *Journal of Hydraulic Engineering*, 141(8), 04015016.
- Evangelista, S., Leopardi, A., Pignatelli, R., and de Marinis, G. (2016). “Closure to “Hydraulic transients in viscoelastic branched pipelines” by S. Evangelista, A. Leopardi, R. Pignatelli, and G. de Marinis.” *Journal of Hydraulic Engineering*, 142(8), 07016006.
- Ferrante, M., Brunone, B., and Meniconi, S. (2009). “Leak detection in branched pipe systems coupling wavelet analysis and a Lagrangian model.” *Journal of Water Supply: Research and Technology – AQUA*, 58(2), 95–106.
- Ferrante, M. and Capponi, C. (2018). “Calibration of viscoelastic parameters by means of transients in a branched water pipeline system.” *Urban Water Journal*, 15(1), 9–15.
- Ghidaoui, M. S., Zhao, M., McInnis, D. A., and Axworthy, D. H. (2005). “A review of water hammer theory and practice.” *Applied Mechanics Reviews*, 58(1), 49–76.
- Huang, Y., Duan, H.-F., Zhao, M., Zhang, Q., Zhao, H., and Zhang, K. (2017). “Probabilistic analysis and evaluation of nodal demand effect on transient analysis in urban water distribution systems.” *Journal of Water Resources Planning and Management*, 143(8), 04017041.

- Jung, B. S., Boulos, P. F., and Wood, D. J. (2007). "Pitfalls of water distribution model skeletonization for surge analysis." *Journal of American Water Works Association*, 99(12), 87–98.
- Jung, B. S., Boulos, P. F., and Wood, D. J. (2009). "Effect of pressure-sensitive demand on surge analysis." *Journal of American Water Works Association*, 101(4), 100–111.
- Keramat, A., Wang, X., Louati, M., Meniconi, S., Brunone, B., and Ghidaoui, M. S. (2019). "Objective functions for transient-based pipeline leakage detection in a noisy environment: Least square and matched-filter." *Journal of Water Resources Planning and Management*, 145(10), 04019042.
- Kim, S. (2016). "Impedance method for abnormality detection of a branched pipeline system." *Water Resources Management*, 30, 1101–1115.
- Meniconi, S., Brunone, B., Ferrante, M., Capponi, C., Carrettini, C., Chiesa, C., Segalini, D., and Lanfranchi, E. (2015). "Anomaly pre-localization in distribution-transmission mains. Preliminary field tests in the Milan pipe system." *Journal of Hydroinformatics*, 17(3), 377–389.
- Meniconi, S., Brunone, B., Ferrante, M., and Massari, C. (2011a). "Potential of transient tests to diagnose real supply pipe systems: What can be done with a single extemporaneous test." *Journal of Water Resources Planning and Management*, 137(2), 238–241.
- Meniconi, S., Brunone, B., Ferrante, M., and Massari, C. (2011b). "Transient tests for locating and sizing illegal branches in pipe systems." *Journal of Hydroinformatics*, 13(3), 334–345.
- Meniconi, S., Brunone, B., and Frisinghelli, M. (2018). "On the role of minor branches, energy dissipation, and small defects in the transient response of transmission mains." *Water*, 10(2), 187.
- USEPA (2006). *Initial distribution system evaluation guidance manual for the final stage 2. Disinfectants and disinfection byproducts rule*. USEPA, Washington.
- Vardy, A. E. and Brown, J. M. B. (1996). "On turbulent, unsteady, smooth pipe friction." *Proc., 7th Int. Conf. on Pressure Surges and Fluid Transients in Pipelines and Open Channels, BHR Group, Harrogate, U.K.*, 289–311.
- Vitkovsky, J. P., Lambert, M. F., Simpson, A. R., and Liggett, J. A. (2007). "Experimental obser-

496 vation and analysis of inverse transients for pipeline leak detection.” *Journal of Water Resources*
497 *Planning and Management*, 133(6), 519–530.

498 Wang, X. J., Lambert, F. M., and Simpson, A. R. (2005). “Behavior of short lateral dead ends on
499 pipeline transients: a lumped parameter model and an analytical solution.” *Journal of Fluids*
500 *Engineering*, 127(3), 529–535.

501 Wood, D. and Chao, S. (1971). “Effect of pipeline junctions on water hammer surges.” *Transporta-*
502 *tion Engineering Journal*, 97(TE3), 441–457.

503

List of Tables

504

1	Umbria region tree-type pipe system – Characteristics of the branches.	23
---	--	----

TABLE 1. Umbria region tree-type pipe system – Characteristics of the branches.

Branch #	D_b (mm)	L_b (m)	s_b (m)	$V_{0,b}$ (m/s)	α	λ	σ	ν
1	263	411	30088	0.41	0.28	0.013	0.99	2.07
2	107.9	203	24915	0.31	0.05	0.007	0.82	1.56
3	312.7	402	21915	0.25	0.40	0.013	0.73	1.24
4	107.9	300	16377	0.14	0.05	0.010	0.54	0.73
5	160.3	178	14381	0.41	0.10	0.006	0.47	2.07
6	160.3	231	11591	0	0.10	0.008	0.38	0
7	210.1	401	10971	0.20	0.18	0.013	0.36	1.03
8	160.3	267	7129	0.31	0.10	0.009	0.23	1.55
9	160.3	257	4513	0.35	0.10	0.008	0.15	1.76
10	150	320	3091	0.10	0.09	0.010	0.10	0.52

List of Figures

1	Single-branch pipe system (Y-system) layout (SR = supply reservoir, EV = end maneuver valve, M = measurement section, b = branch, d = pipe downstream of the junction).	25
2	Frictionless model (FL) – Comparison between the single pipe (SP) and the inactive branch pipe system (IB): pressure signals for different branch characteristics.	26
3	Frictionless model (FL) – Comparison between the single pipe (SP) and the inactive branch pipe system (IB): the determination coefficient, R_{IB}^2 , vs. λ and α , for a given σ ($= 0.5$).	27
4	Frictionless model (FL) – Comparison between the single pipe (SP) and the inactive branch pipe system (IB): the determination coefficient, R_{IB}^2 , vs. λ and σ , for a given α ($= 0.282$).	28
5	Frictionless model (FL) – Comparison between the single pipe (SP) and the inactive branch pipe system (IB): the determination coefficient, R_{IB}^2 , vs. σ and α , for a given λ ($= 0.05$).	29
6	Comparison between the single pipe (SP) and the inactive branch pipe system (IB). Pressure signals in the case of a) the frictionless model (FL), b) the complete model (UF).	30
7	Complete model (UF) – Comparison between the single pipe (SP), the inactive (IB) and the active branch pipe system (AB), with $\nu = 1, 1.5, 2$: the determination coefficient, R^2 , vs. σ and λ , for a given α ($= 0.398$).	31
8	Numerical simulations by the complete model (UF) compared with the fitting by Eq. (15) in the case of the inactive branch pipe system (IB): the determination coefficient R_{IB}^2 , and b) the residuals vs. α and $\lambda + \sigma$	32
9	Numerical simulations by the complete model (UF) compared with the fitting by Eq. (17) in the case of the active branch pipe system (AB), for $\nu = 1$: a) the determination coefficient R_{AB}^2 , and b) the residuals vs. α and σ	33

532	10	Umbria region tree-type pipe system – Sketch of the system (SR and EV indicate	
533		the supply reservoir and the downstream end maneuver valve, respectively; note	
534		that a different length scale has been used for the main pipe and minor branches). . .	34
535	11	Umbria region tree-type pipe system – a) R^2 values given by Eqs. (15) and (17)	
536		for each of the ten branches; b) R_{RS}^2 values given by Eq. (18) vs. the relative	
537		computational time.	35
538	12	Umbria region tree-type pipe system – Comparison between the pressure signals in	
539		the real system, in the single pipe (SP) and in the skeletonized systems. The inset	
540		shows a magnification of these pressure signals in the first period.	36

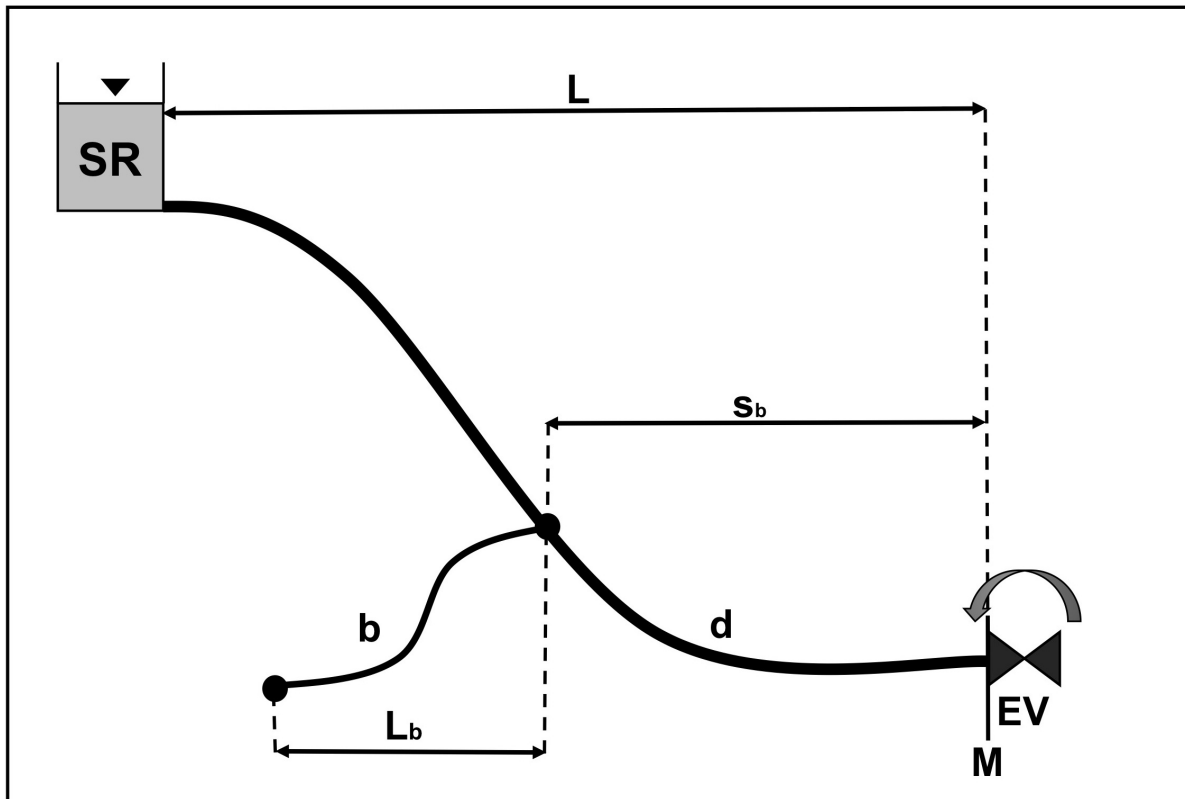


Fig. 1. Single-branch pipe system (Y-system) layout (SR = supply reservoir, EV = end maneuver valve, M = measurement section, b = branch, d = pipe downstream of the junction).

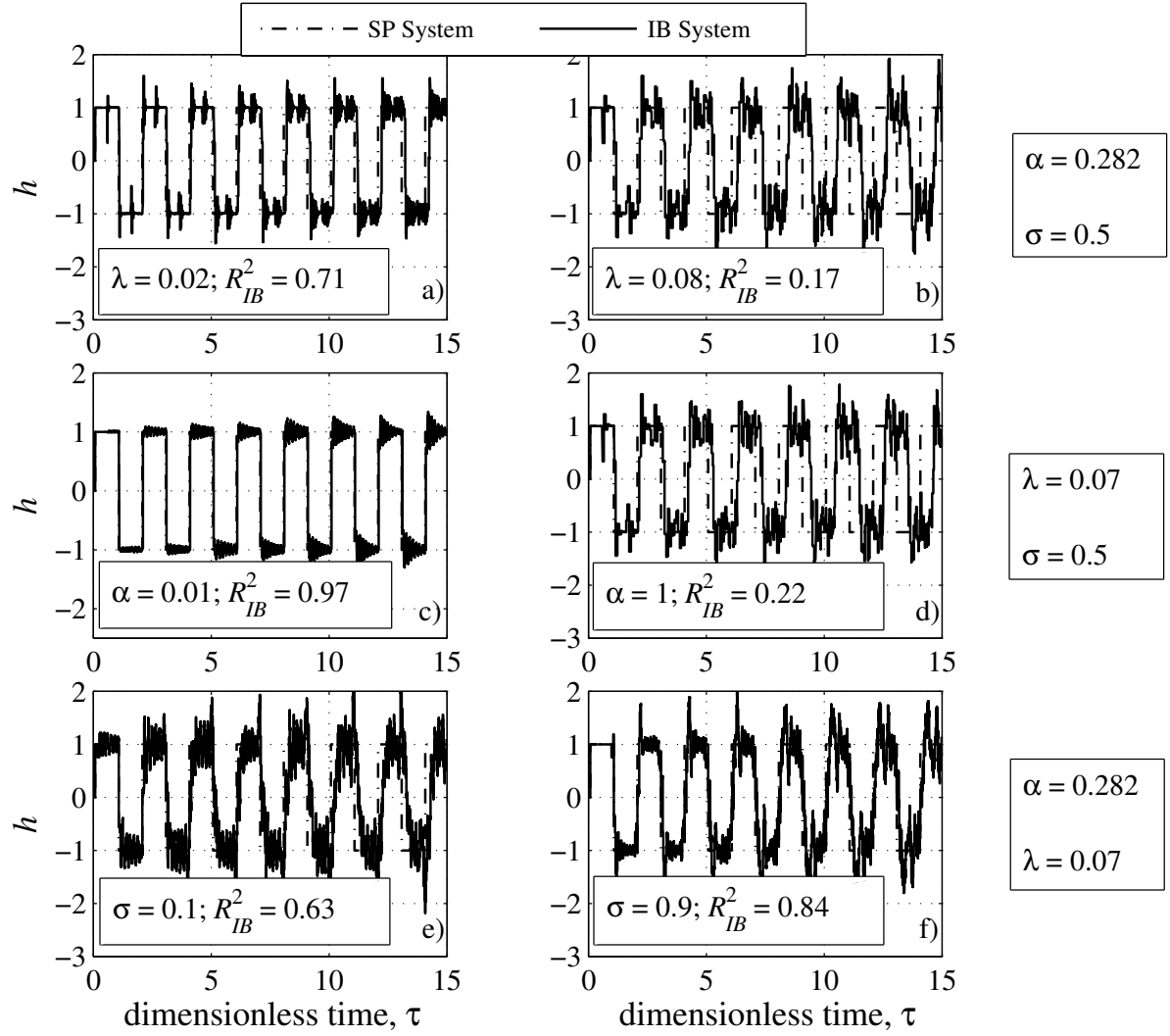


Fig. 2. Frictionless model (FL) – Comparison between the single pipe (SP) and the inactive branch pipe system (IB): pressure signals for different branch characteristics.

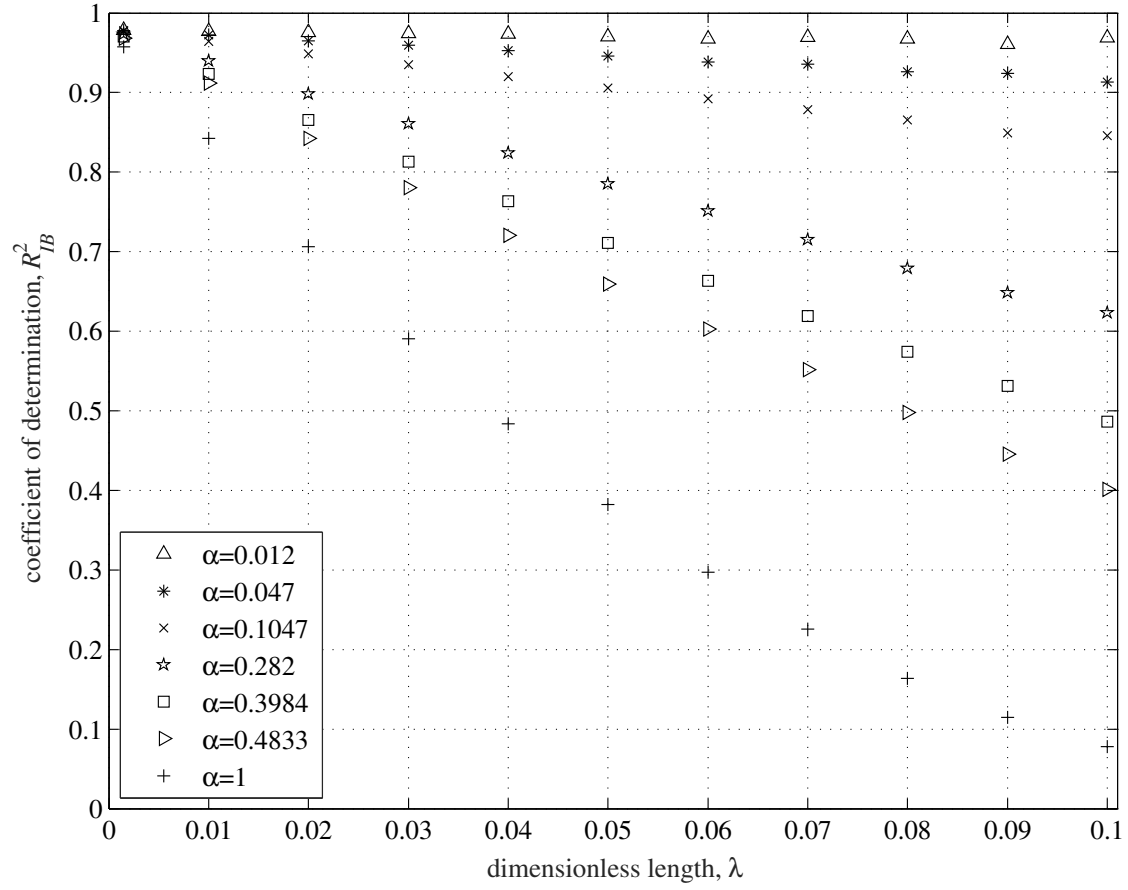


Fig. 3. Frictionless model (FL) – Comparison between the single pipe (SP) and the inactive branch pipe system (IB): the determination coefficient, R^2_{IB} , vs. λ and α , for a given σ ($= 0.5$).

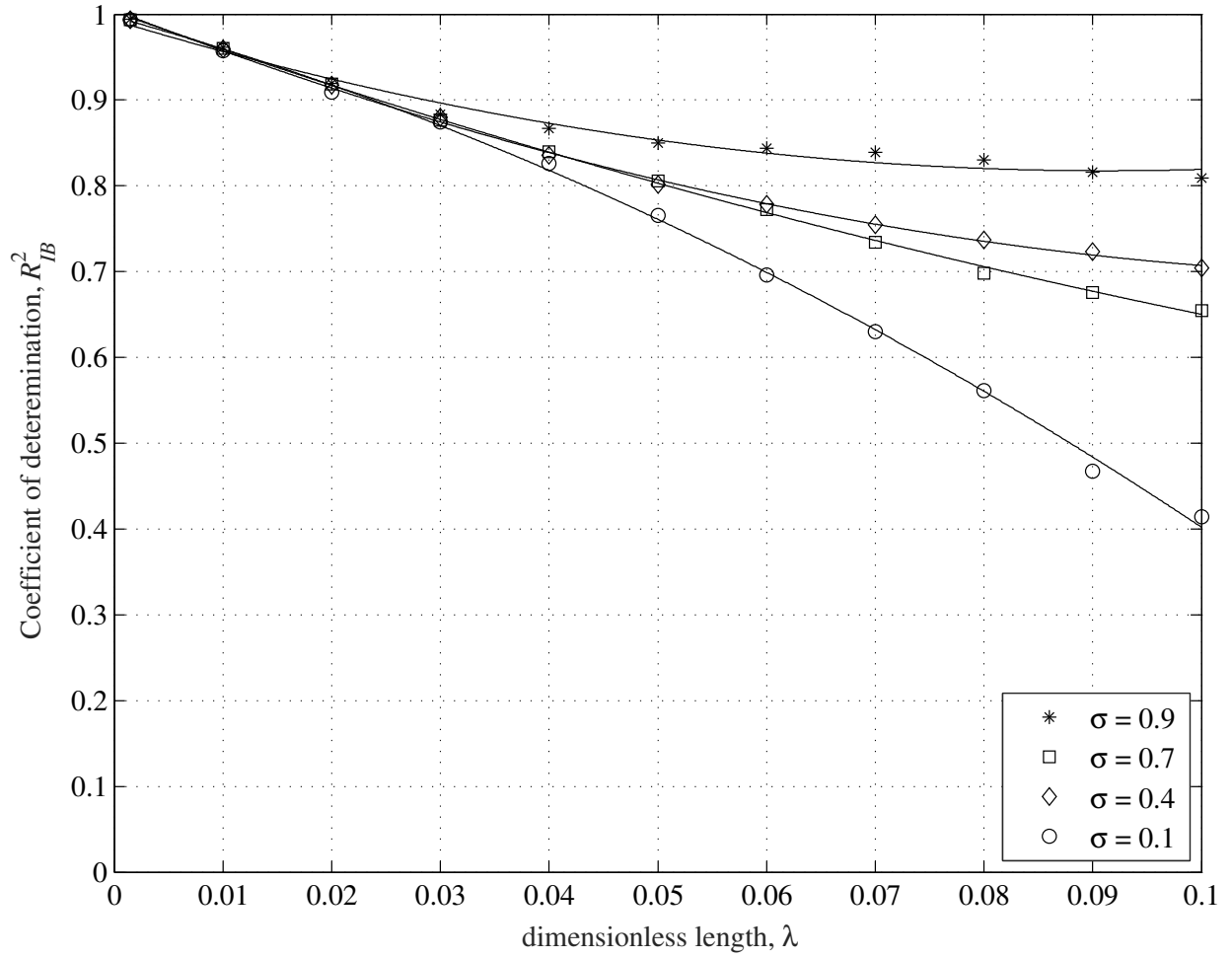


Fig. 4. Frictionless model (FL) – Comparison between the single pipe (SP) and the inactive branch pipe system (IB): the determination coefficient, R^2_{IB} , vs. λ and σ , for a given α ($= 0.282$).

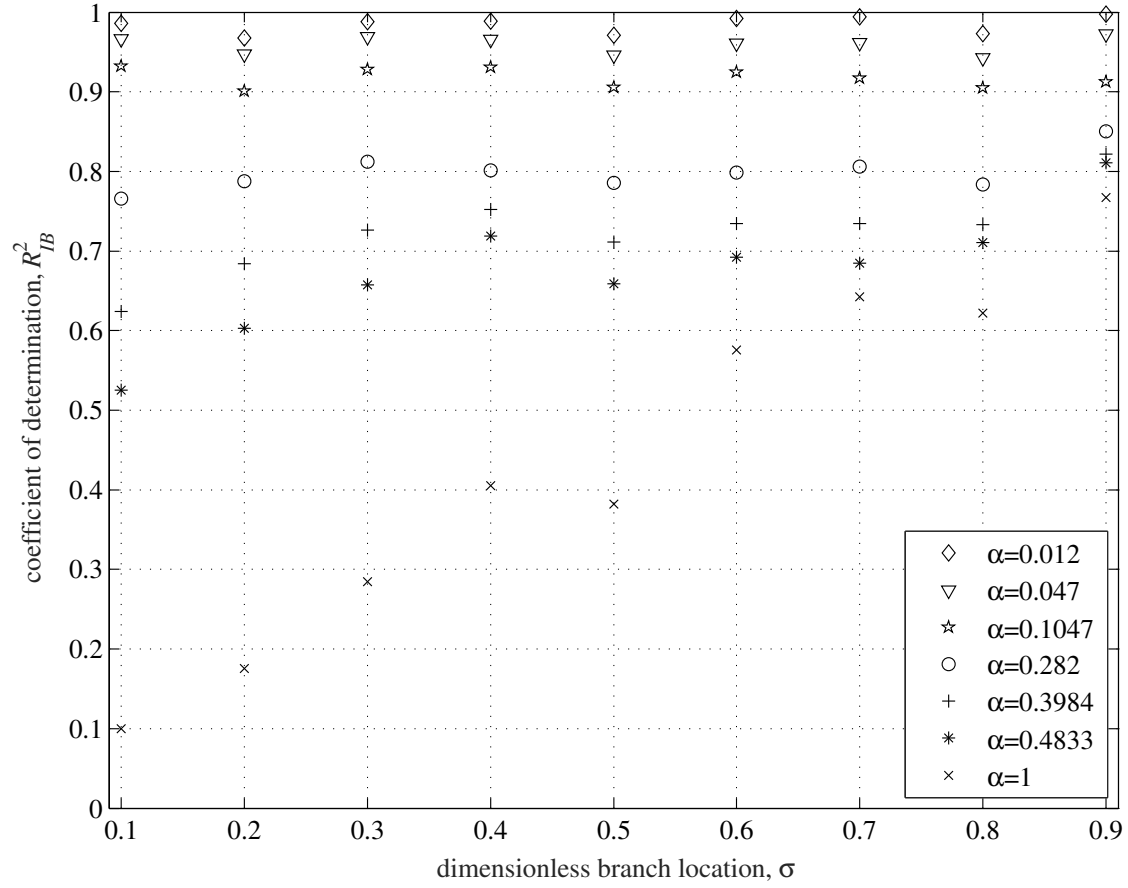


Fig. 5. Frictionless model (FL) – Comparison between the single pipe (SP) and the inactive branch pipe system (IB): the determination coefficient, R^2_{IB} , vs. σ and α , for a given λ ($= 0.05$).

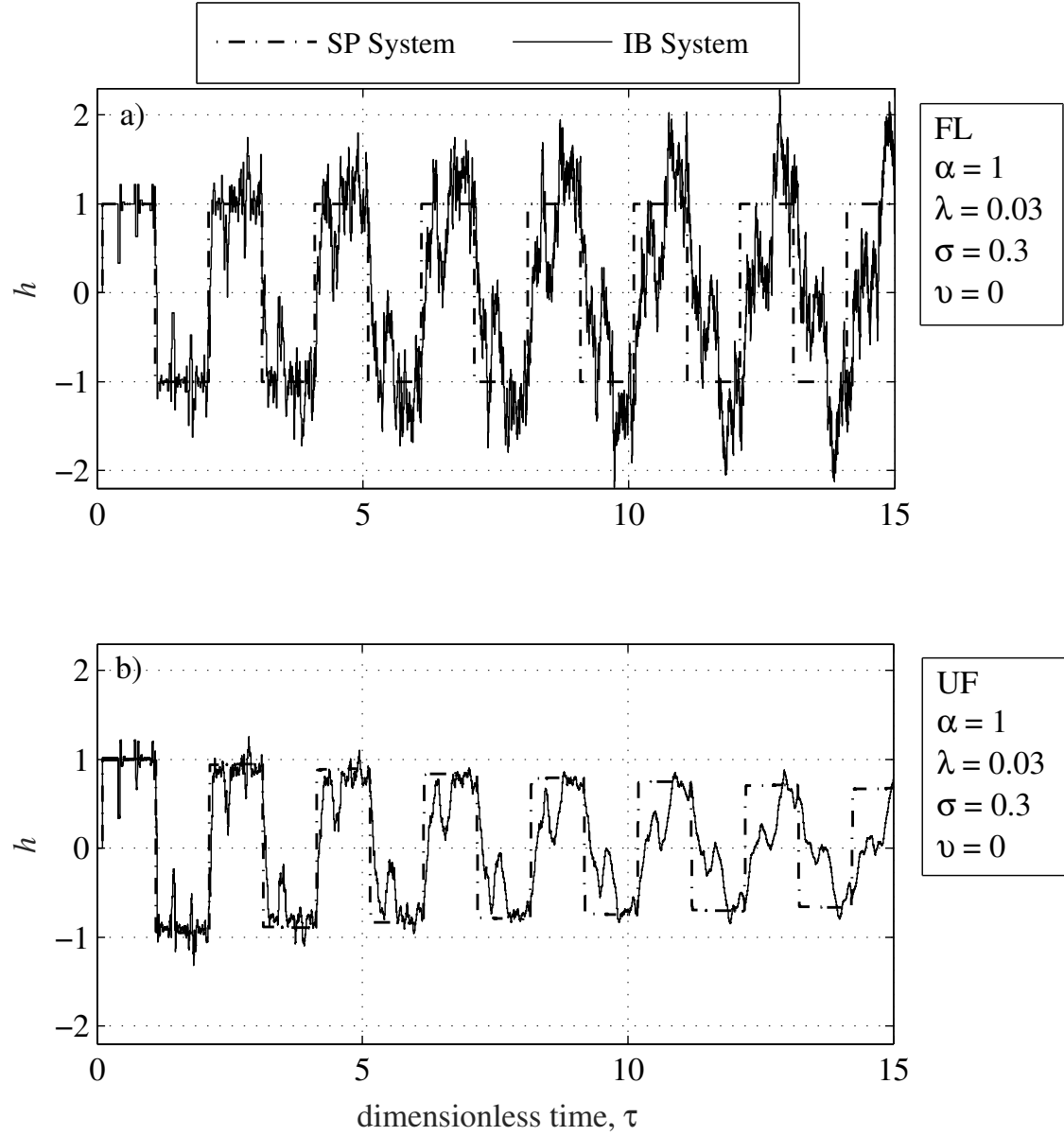


Fig. 6. Comparison between the single pipe (SP) and the inactive branch pipe system (IB). Pressure signals in the case of a) the frictionless model (FL), b) the complete model (UF).

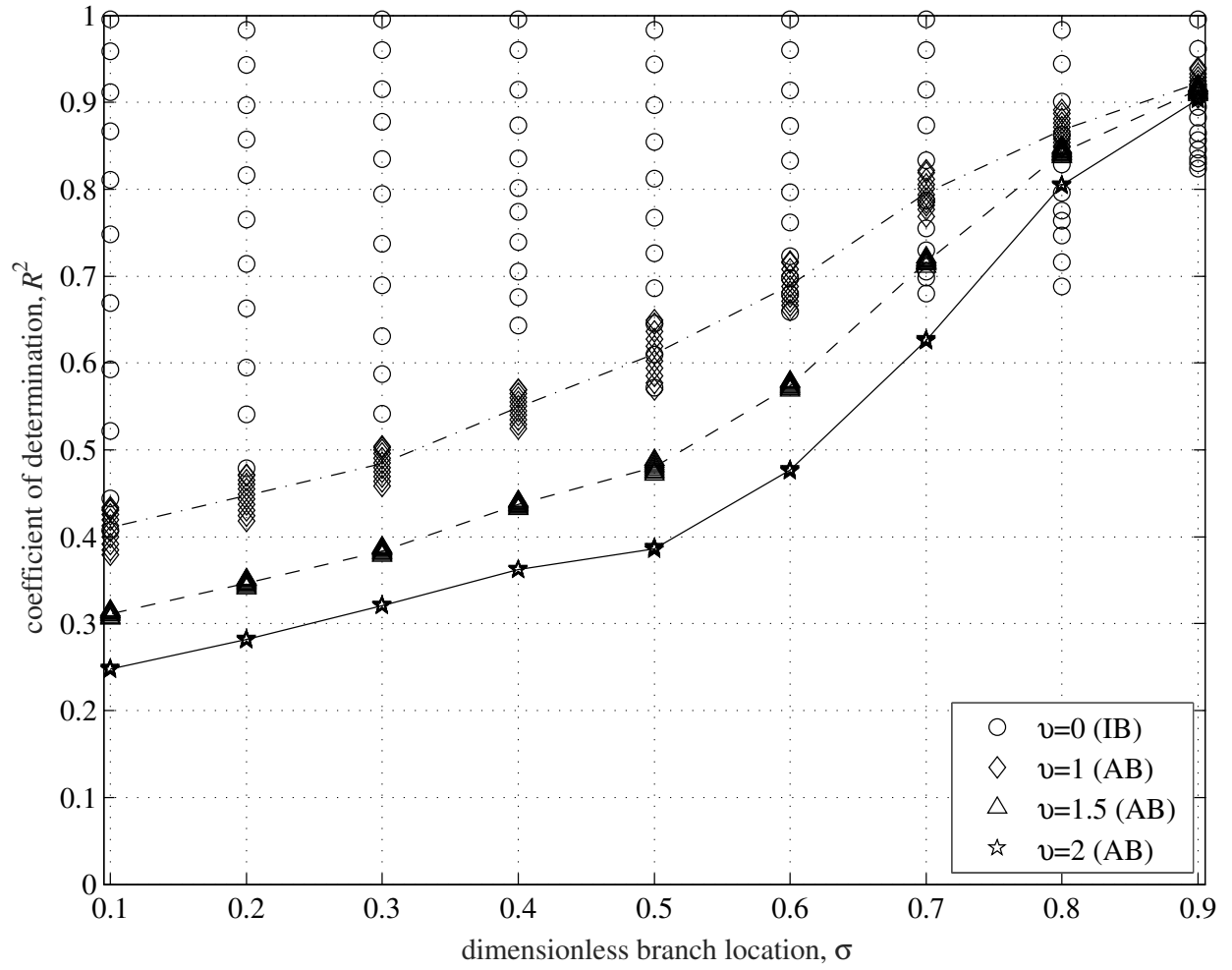


Fig. 7. Complete model (UF) – Comparison between the single pipe (SP), the inactive (IB) and the active branch pipe system (AB), with $\nu = 1, 1.5, 2$: the determination coefficient, R^2 , vs. σ and λ , for a given α ($= 0.398$).

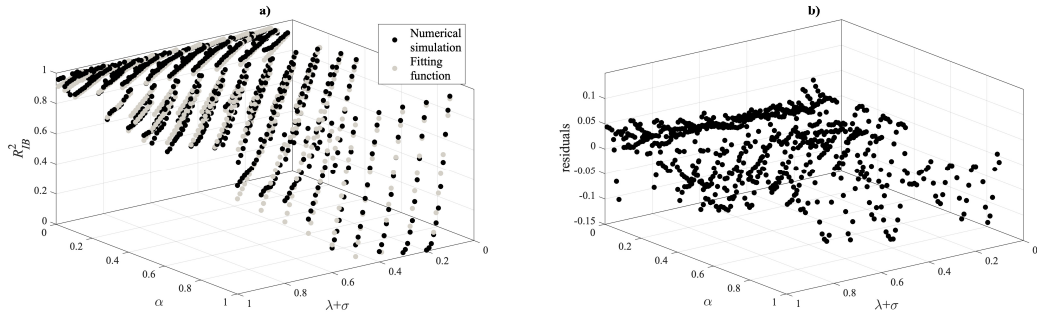


Fig. 8. Numerical simulations by the complete model (UF) compared with the fitting by Eq. (15) in the case of the inactive branch pipe system (IB): the determination coefficient R^2_{IB} , and b) the residuals vs. α and $\lambda + \sigma$.

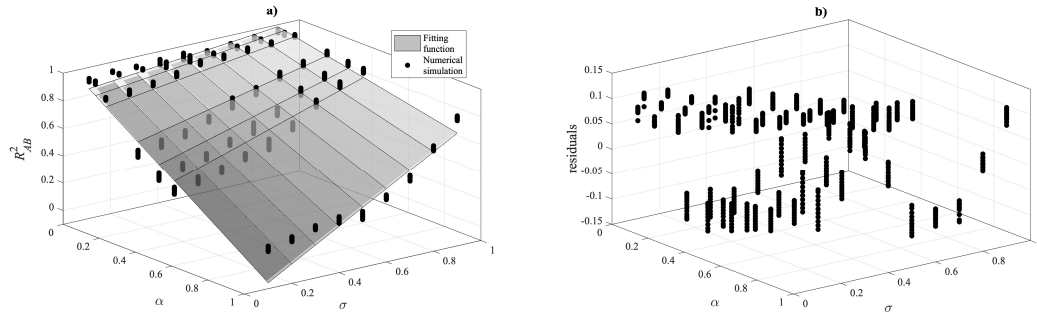


Fig. 9. Numerical simulations by the complete model (UF) compared with the fitting by Eq. (17) in the case of the active branch pipe system (AB), for $\nu = 1$: a) the determination coefficient R_{AB}^2 , and b) the residuals vs. α and σ .

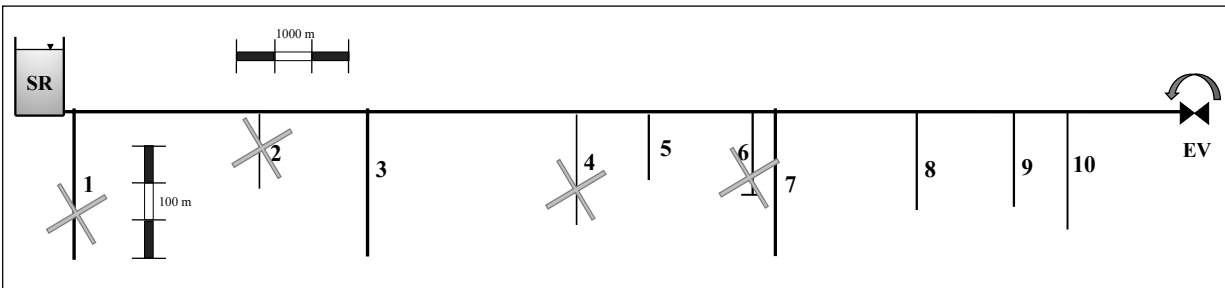


Fig. 10. Umbria region tree-type pipe system – Sketch of the system (SR and EV indicate the supply reservoir and the downstream end maneuver valve, respectively; note that a different length scale has been used for the main pipe and minor branches).

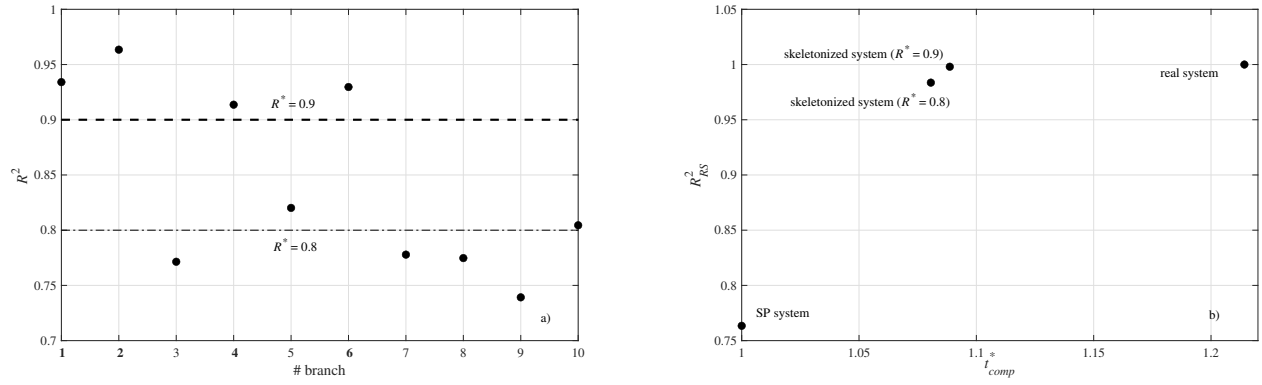


Fig. 11. Umbria region tree-type pipe system – a) R^2 values given by Eqs. (15) and (17) for each of the ten branches; b) R^2_{RS} values given by Eq. (18) vs. the relative computational time.

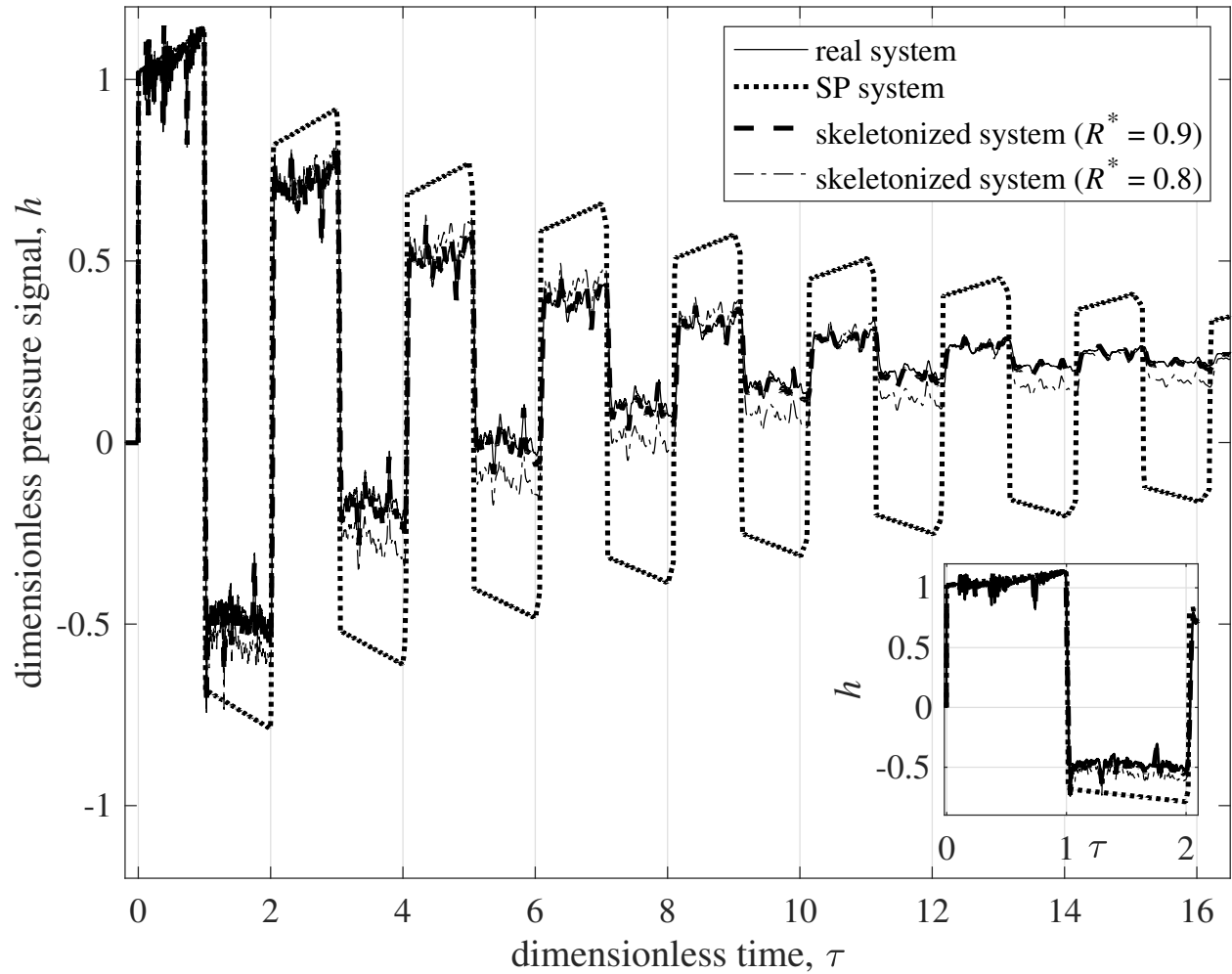


Fig. 12. Umbria region tree-type pipe system – Comparison between the pressure signals in the real system, in the single pipe (SP) and in the skeletonized systems. The inset shows a magnification of these pressure signals in the first period.